CFD studies on the high-viscosity oil-water two-phase flow in a horizontal pipe

Cite as: AIP Conference Proceedings **2654**, 040014 (2023); https://doi.org/10.1063/5.0114228
Published Online: 14 February 2023

Bahrul Jalaali, Eli Kumolosari and Okto Dinaryanto

CFD Studies on the High-Viscosity Oil-Water Two-Phase Flow in a Horizontal Pipe

Bahrul Jalaali[1)], Eli Kumolosari[1)], and Okto Dinaryanto[1, a)]

[1]*Department of Mechanical Engineering, Faculty of Aerospace Technology, Institut Teknologi Dirgantara Adisutjipto, Yogyakarta, Indonesia*

[a)] Corresponding author: okto.dinaryanto@mail.ugm.ac.id

Abstract. In order to enhance the understanding of co-current oil-water flow behavior in a horizontal pipe, CFD studies of the oil-water transient model flow were carried out. In the present work, the flow simulation was solved numerically using Volume-of-Fluid (VoF) multiphase model while the turbulence model was performed using the SST k-ω. In addition, the viscosity of oil was sensitive to the temperature changes that influenced the changes in flow patterns. Therefore, the energy equation solver was also activated to observe the flow changes due to this case. The oil and water superficial velocity ranges were between 0.06-0.4 m/s and 0.18-0.81 m/s. The water flow temperatures were varied by 300K and 373K. The oil-water density was adjusted to have approximately matched values while a medium API for the oil characteristic model was selected. The computational domain was observed on a pipe with 26mm in diameter and 1m in length for the primary pipe, while the oil and water inlets diameter were set to 12mm. A comparison with experimental data showed relatively good agreement, both qualitative and quantitative. Furthermore, the flow characteristics were obtained with satisfactory predictions in particular different flow regimes. Here, the quantitative results of oil volume fraction were investigated as well. This study also found that increasing temperature affected flow behavior and transformed the oil lumps in water flow pattern into the stratified flow. Moreover, the numerical simulation appeared to be a reliable tool for predicting oil-water flow characteristics and investigating the influence of temperature in the flow.

INTRODUCTION

Liquid-liquid multiphase flows are ubiquitous phenomena that appear in many industrial processes and the petroleum industry. The flow within the pipe can acquire various flow distribution characteristics in terms of flow regimes [1]. Here, oil-water flow patterns are necessary to observe for its transport purposes. Previous methods have been conducted to obtain the multiphase flow characteristic by various experimental procedures [2,3] and image processing [4,5]. Several studies also revealed that flow patterns in an oil-water took into account some parameters such as velocities, densities, and viscosities [1,6]. Those of the two latter are sensitive to temperature changes [7]. In particular, considering the temperature effect that might convert the flow patterns into other forms, predicting flow patterns is essential to calculate the pressure drop along the pipe and determine the facilities' optimum design and maintenance [6]. The temperature parameter should further be investigated following the changes in flow characteristics.

The observed flow patterns of oil-water flow are mainly classified as stratified flow, annular flow, and dispersed flow [1,2]. The stratified flow appears in separated layers of oil-water despite their different density. The dispersed flow is one fluid on continuous flow while the other is in the form of dispersed. Moreover, when both liquids have resembled densities, the core annular flow is recognized [1]. The flow pattern observed in oil-water was strongly influenced by physical phenomena, whereas further studies revealed the flow pattern based on density and viscosity. The study of Charles et al. [8] was conducted in the case of low-viscosity oil and liquids equal densities. The pattern of water in oil emulsion, oil slug/plug in water, oil drops in water, annular flow, and oil in water emulsion were obtained. Trallero et al. [3] and Nadler and Mewes. [9] investigated upon low-viscosity oil but unequal densities. Most

Proceedings of the 7th International Conference on Science and Technology
AIP Conf. Proc. 2654, 040014-1–040014-14; https://doi.org/10.1063/5.0114228
Published by AIP Publishing. 978-0-7354-4315-0/$30.00

flow patterns were constructed by stratified flow, whereby stratified with dispersion and mixing were also found. An experimental study of high viscosity and equal densities was done by Shi and Yeung. [10]. The flow was investigated where some additional flow patterns were noticed: annular flow, oil plugs, oil lumps in water, and dispersed oil. Based on the aforementioned studies, experimental studies were necessary to produce the flow pattern characteristic of oil-water flow. Due to its dependence on physical phenomena, flow patterns data must be generated in a wide variety. Unfortunately, it also increases the cost because of the experiment's needs. For that reason, an alternative technique should be provided to surpass that obstacle. Furthermore, the widely used computational study is considered as another way to investigate the flow characteristic.

Previous studies of CFD in analyzing multiphase flow were conducted by Shi et al. [11]. The results were compared to the experimental results with satisfactory outcomes. It was worth noting that the predicted oil fouling film was susceptible to the wall contact angle; hence it should be pointed out in the further study. Deendarlianto et al. [12] studied the multiphase plug flow using CFD calculation while the results were in good agreement with the experimental data. It found that the liquid flow mechanism increased due to the higher gas superficial velocity. Jalaali and Pranowo. [13] utilized the non-conventional method of CFD and provided an adequate result of flow characteristics in liquid-liquid mixing. It revealed that density and viscosity tended to influence the liquid mixing phase. Tan et al. [14], conducted the study of phase inversion point case on the liquid-liquid flow. The water-lubricated flow on the oil-water was considered to reduce the pressure drop, while viscosity effects were analyzed on the flow characteristic. Furthermore, the effect of viscosity related to the flow characteristic was also found in the works of Yuana et al. [15] and Jalaali et al. [16]. It was described that flow characteristic was highly influenced by density and viscosity ratio. Medium and high viscosity oil-water flow was simulated by Shi et al. [11] and Shi et al. [17]. The model of VoF k-ω was applied and resulted in satisfying results compared to the experimental. The annular flow pattern characteristics were profoundly observed through CFD results. Another study by Dehkordi et al. [18] discussed the stratified flow of oil-water. The core annular flow was observed, and the predicted result of CFD data was in line with the experimental. Evgenii et al. [19] numerically studied the vertical flow of oil in water flow. The Lagrangian method was utilized, and the results were also in good agreement with those of analytical prediction. From the previous explanation, it was evident that CFD has capabilities to simulate the horizontal and vertical flow numerically. However, to the best authors know, the study of the temperature effect in oil-water flow on the horizontal pipe is still scarce.

In general, CFD is a robust technique for simulating the multiphase phenomena. In this study, we compare the experimental and CFD results of a particular oil-water flow in a horizontal pipe. The experimental result cites from previous studies to validate the results whereby the temperature parameter is added in examining the flow characteristic related to the flow pattern changes. Furthermore, this study intends to be an initial investigation of the consideration of temperature on the oil-water flow. This paper organizes as follows: computational modeling elaborates in Sec.2, the results are discussed in Sec.3, and the conclusion is presented in Sec.4.

COMPUTATIONAL MODELING

In this simulation, the volume-of-fluid (VoF) model was used to track the interface between multiphase fluid. This method was the Eulerian method whereby the fluid was observed through a fixed computational domain. This model was clearly adequate to observe multiphase phenomena as stated in Refs. [11, 12, 14]. Hence, this study employed this model. The fluid analysis is based on mass and momentum conservation as described in Eqs. (1) and (2). Where ρ and u are the density (kg/m^3) and the velocity (m/s). Moreover, $\boldsymbol{u}^T$ and $\boldsymbol{g}$ denote the turbulent velocity (m/s) and gravitational acceleration (m/s^2).

$$\frac{\partial(\rho)}{\partial t} + \nabla.(\rho.\boldsymbol{u}) = 0 \quad (1)$$

$$\frac{\partial}{\partial t}(\rho\boldsymbol{u}) + \nabla.(\rho\boldsymbol{u}.\boldsymbol{u}) = -\nabla p + \nabla.[\mu(\nabla\boldsymbol{u} + \nabla\boldsymbol{u}^T)] + \rho\boldsymbol{g} + \boldsymbol{F} \quad (2)$$

Furthermore, the equation of VoF is shown in Eq. (3). This model is used to accomplish the interface track by solving the volume fraction of the primary phase. The criteria of the interface were determined by calculating the volume fraction of both fluids; meanwhile, volume fraction of each fluid was tracked through every computational grid. The physical properties of the mixture, such as density and viscosity, were weighted by the volume fraction in the presence of control volume, as shown in Eqs. (4) and (5). The total volume fraction was unified to be 1 ($\alpha_w + \alpha_o = 1$). The term of α was a volume fraction whereby the subscript of o and w represents the 'oil' and 'water'. In this study, water was the primary phase, while oil was the second phase. Moreover, the body force included in the

momentum equation resulted from the existence of the interface. The following body force was used by utilizing a correlation of Brackbill et al. [20] as continuum surface flow (CST), stated in Eq. (6).

$$\frac{\partial(\rho_o \alpha_o)}{\partial t} + \nabla.(\rho_o \alpha_o u) = 0 \quad (3)$$

$$\rho = \alpha_o \rho_o + \alpha_w \rho_w \quad (4)$$

$$\mu = \alpha_o \mu_o + \alpha_w \mu_w \quad (5)$$

$$\boldsymbol{F} = \sigma \nabla. \frac{\nabla \alpha_o}{\|\nabla \alpha_o\|} \frac{\rho \nabla \alpha_o}{\frac{1}{2}(\rho_o + \rho_w)} \quad (6)$$

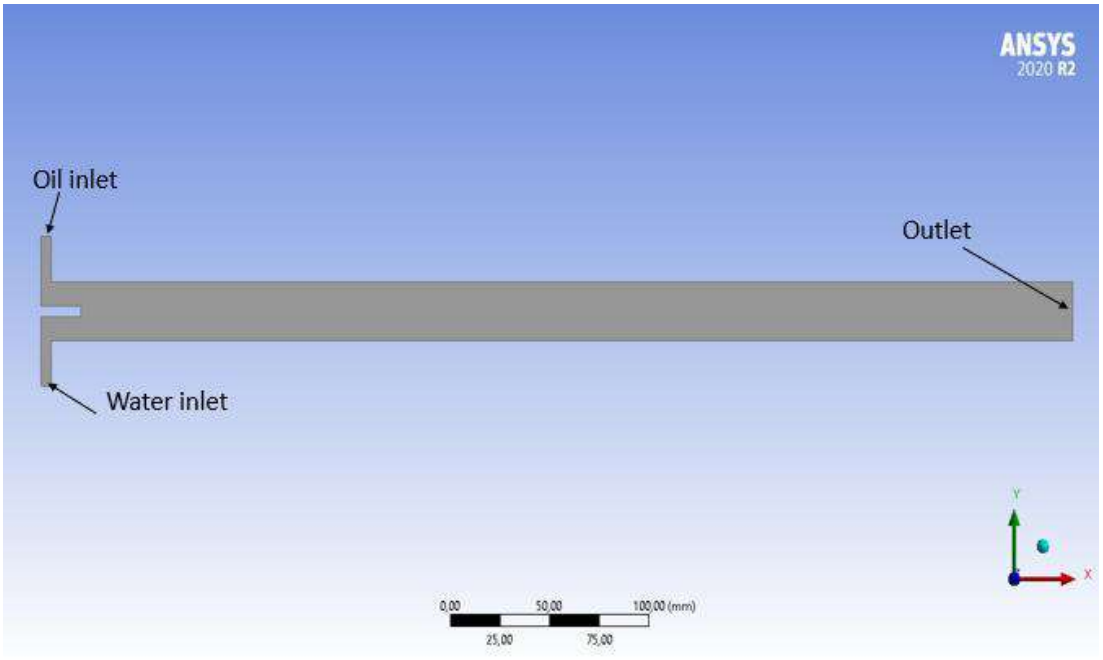

FIGURE 1. Computational domain

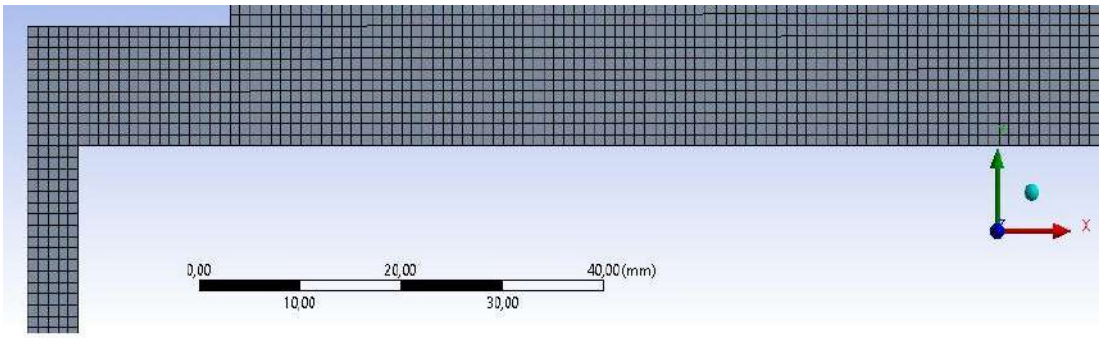

FIGURE 2. Representative of generated mesh.

Here, the geometry model was composed of two inlets which were respectively the oil and water inlets. The representative figure of geometry is shown in Fig. 1 and 2. The separation 5mm plat was mounted between those inlets to separate the fluids flow entirely before entering the main pipe. The inlet diameter and main pipe diameter were set to 13mm and 26mm, while the length of the main pipe was 1m. The initial values of nominal water and oil viscosity were μ_w: 1cP and μ_o: 5000 cP, whereby the densities of water and oil were ρ_w: 998 kg/m^3 and ρ_o: 910 kg/m^3. Based on Alomair et al. [7], the value of viscosity and density was approximated into a polynomial function. The properties of water and oil by means of temperature effect were conformed using user-defined function (UDF) input. This setup was done so that the effect of temperature related to the flow characteristic could be observed. In terms of

temperature effect, the energy equation (Eq. 7) was coupled in the calculation by activating the energy equation setup. The water temperature inputs were varied at 300K and 373K. The surface tension between the fluids was adjusted, σ: 0.02 N/m. The water (U_{sw}) and oil (U_{so}) superficial velocity was adapted in between 0.06 – 0.4 m/s and 0.1 – 0.81 m/s, respectively. The kinetic and potential energy was neglected. A further summary of numerical parameters is shown in Table 1.

$$\frac{\partial}{\partial t}(\rho E) + \nabla.\left(\boldsymbol{u}(\rho E + p)\right) = \nabla.\left(k_{eff}\nabla T - \sum_j h_j \boldsymbol{J_j} + \left(\bar{\bar{\tau}}_{eff}.\boldsymbol{u}\right)\right) + \boldsymbol{S_h} \quad (7)$$

TABLE 1. Numerical parameters for the simulation

Simulation parameters	Selection
Type of analysis	Transient
Time step adjustment	Fixed, max (Courant number) < 0.25
Simulation time step	0.1s
Total simulation time	40s
Transient scheme	First order implicit
Turbulent numeric	First order

The velocity boundary and pressure outlet were set up at the inlets and outlet, respectively. The observation was conducted at the point where both fluids attained the fully developed flow. The no-slip boundary condition was imposed at the wall adhesion while the value of contact angle, θ_{wl} = 175º, was adopted based on Shi et al. [11]. The transient flow was applied and solved using the pressure-based algorithm where explicit approximation was utilized. Furthermore, to solve the pressure interpolation and pressure-velocity coupling, the PRESTO! and SIMPLE scheme were used, respectively. This selection was intended to increase the numerical result, as cited from Shi et al. [11]. The pressure staggering option (PRESTO!) uses the discrete continuity balance to compute pressure on staggered control volume [21]. It gives more accurate results since the error of interpolation was avoided by neglecting the pressure gradient assumption [22]. The semi-implicit method for pressure-linked equation (SIMPLE) was subsequently utilized since this algorithm has more skewness correction [21]. The momentum equation was solved with upwind 1st order while the time-step and the convergence criteria were set to 0.1s and 10^{-5}.

In this numerical study, modeling was conducted in 2D approximation. The quadrilaterals structured mesh for the entire flow field inside the pipe was handled. It was chosen so that a refined grid could be acquired since structured mesh was easier to be refined. The grid height value was determined by calculating based on the y^+ parameter, which was the criteria of grid height towards the boundary layer [21]. The value y^+ is expressed in Eq. 8 whereby y is the grid height and τ_w is the wall shear stress [21]. In this work, the y^+ value was set to < 30 according to the Fluent turbulence guide [21]. Based on the calculation. it was obtained that the minimum value of grid height (y) was 7.4mm. In order to capture more accurate results on the fluid characteristic at an adjacent wall and the interface, the smaller cell height was considered. Thus, the grid size was investigated by examining the optimum simulation results of the element size between 4mm, 2mm, and 1mm. The inflation mesh was not utilized since it was 2D computational. The computational time of 2D simulation was faster than 3D hence numerical duration was not becoming an obstacle in the calculation process. Thus, in the entire domain, a refined grid was handled.

$$y^+ = \frac{y\sqrt{\frac{\tau_w}{\rho}}\rho}{\mu} \quad (8)$$

The sensitivity analysis, known as the demonstration of grid independence, was performed. It considered that the value of the solution remained the same when the grids were refined. The smaller grid size is intended to be more accurate in terms of capturing boundary layer phenomena. This became important since the interaction of oil-water with the pipe wall influenced the flow patterns. The quantitative result of oil volume fraction comparison between experimental, cited from Shi and Yeung. [10], and simulation result was considered. Furthermore, visual validation was also observed in the validation step. The observed visual flow through experimental was compared with the simulation result. The resemble flow visualization determined the benchmarking consideration.

RESULT AND DISCUSSION

Validation result

The CFD studies of oil-water flow were conducted using numerical simulation. Prior to examining the results, the grid independence test was performed. Both quantitative and qualitative benchmarks were implemented. The quantitative result was done by comparing the experimental result of averaged oil volume fraction in the case of U_{so}: 0.12 m/s and U_{sw}: 0.61 m/s. Here, by considering the $y+$ parameter, the simulation result for grid independence shows in Table 2. The experimental result of averaged oil volume fraction was 0.33 [10]. The discrepancy of 4mm, 2mm and 1mm grids values were respectively obtained at about 11%.

The value of $y+$is related to accurately capturing the boundary layer phenomena. Here, based on the calculation, $y+$ value of 1mm grid obtained 1.02 while the value increased at larger grid size. It concluded that the phenomena related to the boundary layer at the adjacent wall and interface might be clearly observed on 1mm. In the next step, visual validation was done to confirm, whereas the visual comparison with the experimental result was further investigated, as shown in Fig. 3. The figure indicates that the brighter image is water while the darker is oil. On the other hand, the simulation results are represented in the color of red and blue color. The water illustrates by blue color while red is the oil. At 1mm grid size, the result produced smother figures than those of 2mm and 4mm hence it produced the most accurate result. The reason was the number of grids, it influenced the visual result, although the oil volume fraction has identical results. It was worth noting that visual observation was necessary for the validation step.

TABLE 2. Benchmarking result of y^+ and averaged oil volume fraction

Grid size	Calculated (y^+)	Averaged oil volume fraction
1mm	1.02	0.301
2mm	15.8	0.307
4mm	30.5	0.307

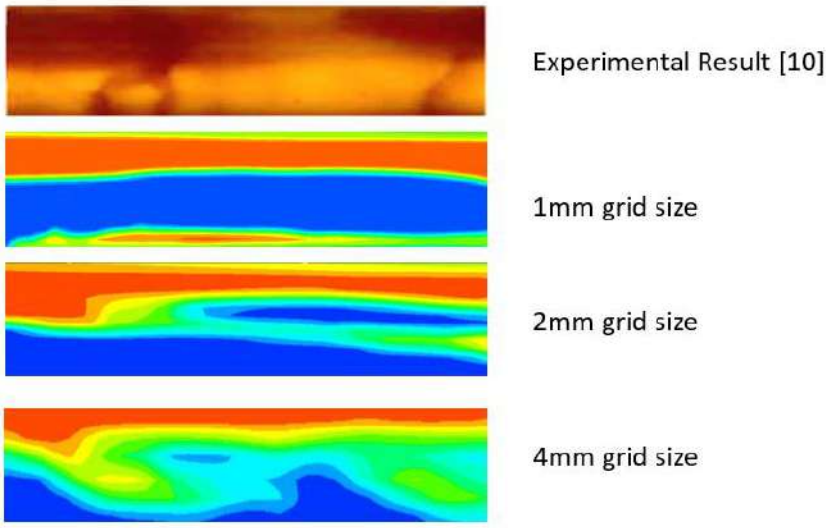

FIGURE 3. Comparison results on particular grid size and experimental [10] result

Flow Regimes

The CFD codes were carried out to simulate the high-viscosity oil-water flow pattern. The results are shown in Fig. 4. In these results, the water was represented by blue color while the red one is the oil. The legend described the oil-volume fraction. The experimental result from a previous study [10] showed a mixture of oil-water, where oil illustrated the darker one. We performed five simulation cases representing each flow regime. For high viscosity oil, the viscous force has a significant effect of preventing break-up oil interface. As shown in Fig. 4, the flow pattern obtained from the simulation can be divided into three basic categories: (1) oil plugs in water; (2) oil lumps in water; (3) core annular flow. The simulation agreed with Shi and Yeung's experiment data [10] for water-continuous high-

viscosity oil-water flow in horizontal pipes. Furthermore, compared with the interfacial structures obtained from the visualization [10,11], the simulation of flow structures agreed with the experimental observation. Figure 4 also enhance the validation that the simulation result produced nearly the same trend outcomes in the visualization. This also showed that the VoF method in the commercial CFD code of FLUENT could simulate the flow pattern of liquid-liquid two-phase flow in a horizontal pipe.

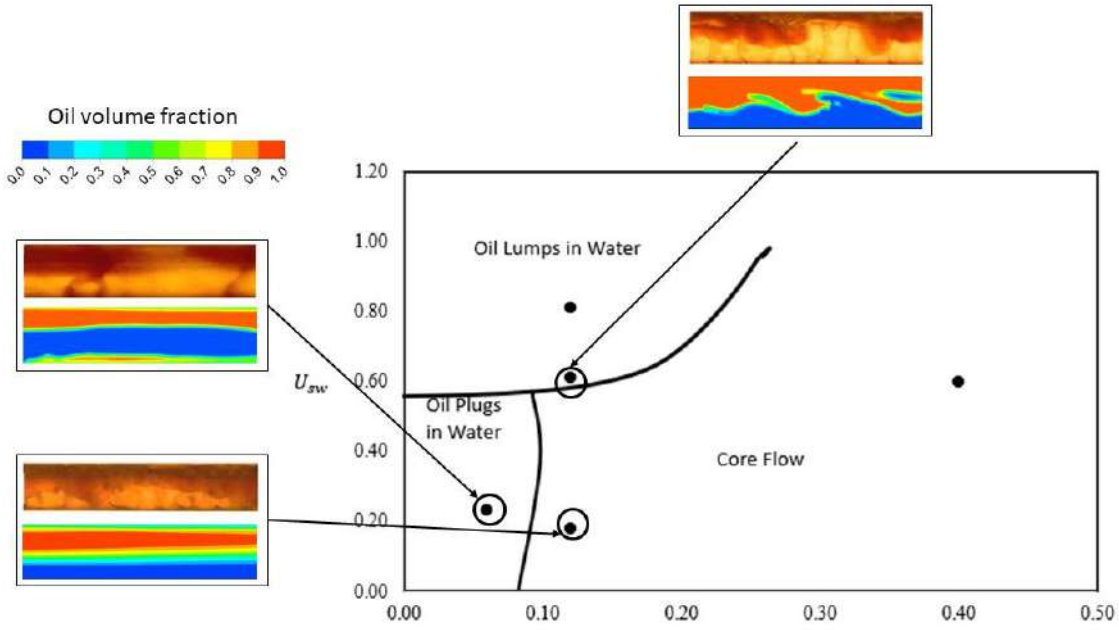

FIGURE 4. Comparison result of CFD (below) model and experimental (above) [9].

Oil plugs in water

Figure 5 shows the example of flow structure obtained from the CFD simulation. At low U_{so} and U_{sw}, the oil plugs in the water flow structure have appeared. For the water velocity = 0.23 m/s and the oil velocity = 0.06 m/s, the simulation flow pattern is characterized by oil plugs in various lengths separated by water. The pattern flow shows that the water blocks to prevent the oil passes in the pipe (Figure 6). Due to the high viscosity of the oil flow, the interfacial tension and viscous force prevent the oil interface break up, and the oil tends to form oil plugs flow. The simulation results agree with the flow pattern from Shi and Yeung [10], Charles et al. [8] experiment result. Next, Figure 7 shows the obtained oil volume fraction data from the simulation that fluctuates periodically, offering low and high-volume fraction values. The oil volume fraction peak represents the oil plug and depends on the passing of oil plugs and water blocked.

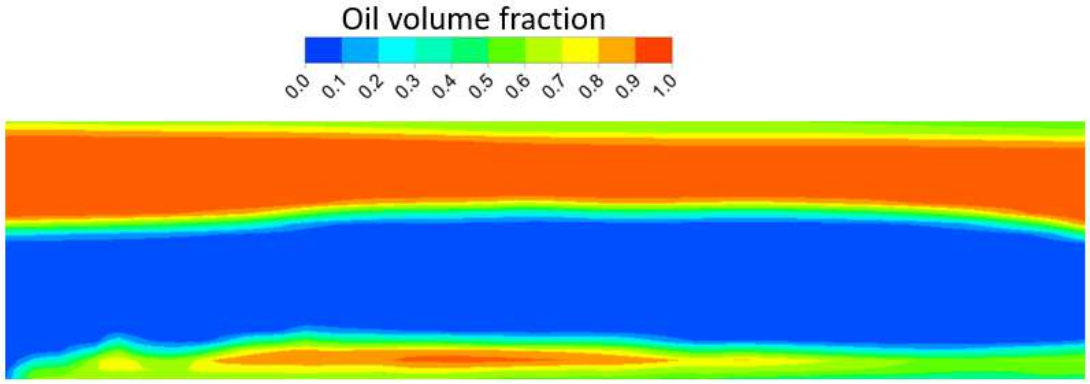

FIGURE 5. Simulation result of Oil Plugs in water in earlier time (U_{so}: 0.06 m/s, U_{sw}: 0.23 m/s)

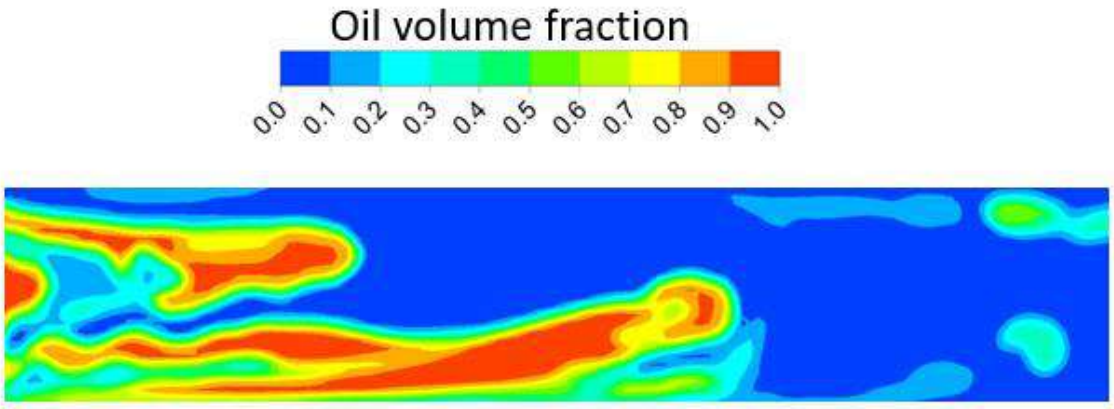

FIGURE 6. Simulation result of Oil Plugs in water in later stage (U_{so}: 0.06 m/s, U_{sw}: 0.23 m/s)

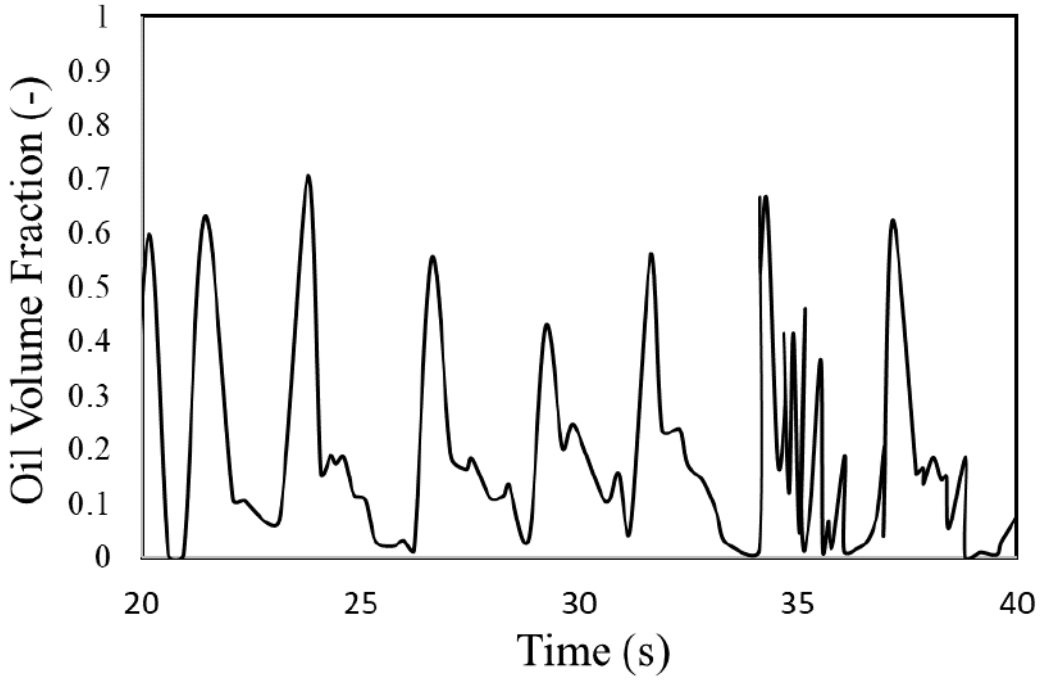

FIGURE 7. Oil volume fraction of Oil Plugs in water (U_{so}: 0.06 m/s, U_{sw}: 0.23 m/s).

Oil lumps in water

At a higher water velocity, where U_{sw}: 0.61 m/s and U_{so}: 0.12 m/s, the simulation results show that the flow pattern is dominated by oil lumps in various shapes separated by water shown in Figure 8. As water velocity increases, the oil plugs tend to split up due to the rise of the water inertia flow. The simulation also shows that the oil lump tends to be break-up as water velocity increases, as shown in Figure 10. The simulation results agree with the Shi and Yeung [10] experiment result. Next, figures 9 and 11 show that the oil volume fraction of oil lumps in water patterns has a lower value than oil plugs patterns. The oil volume fraction peak represents the oil lump. As the water velocity increases, the fluctuation of the oil volume fraction also increases, as shown in Figures 11.

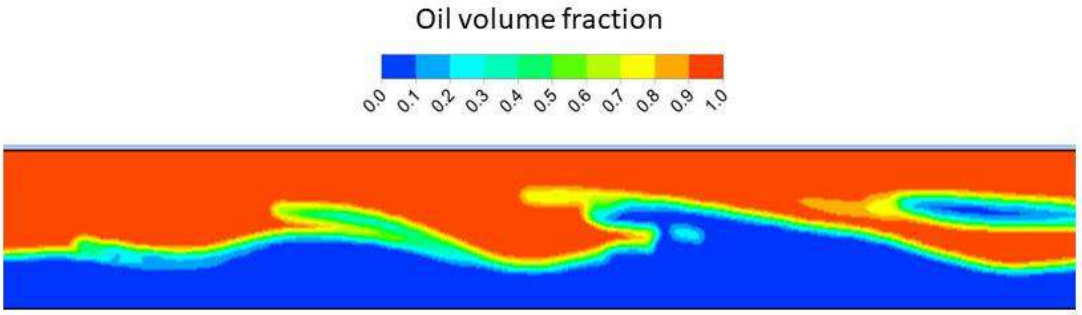

FIGURE 8. Simulation result of Oil Lumps in water (U_{so}: 0.12 m/s, U_{sw}: 0.61 m/s).

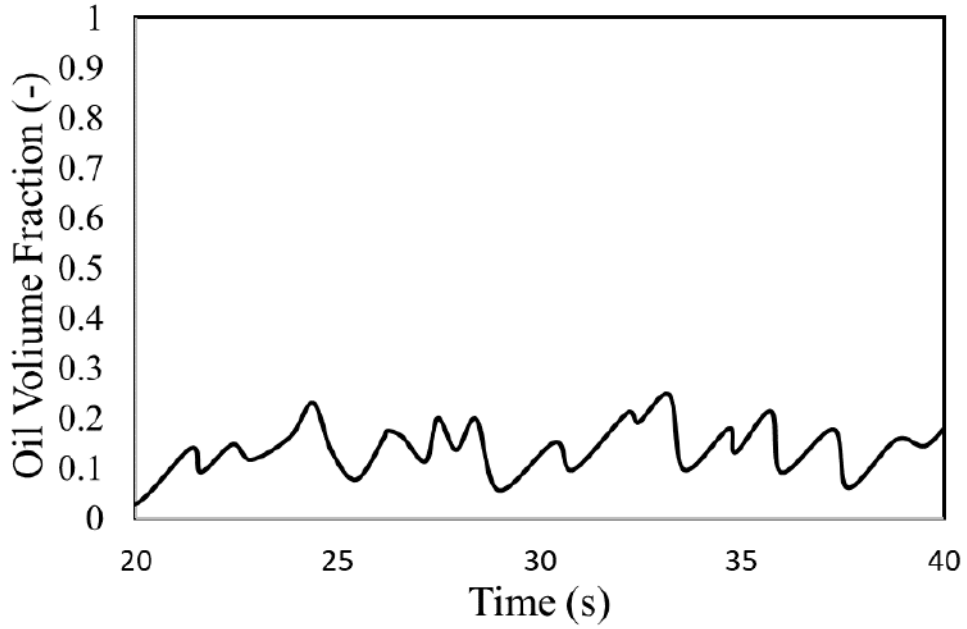

FIGURE 9. Oil volume fraction of Oil Lumps in water (U_{so}: 0.12 m/s, U_{sw}: 0.61 m/s).

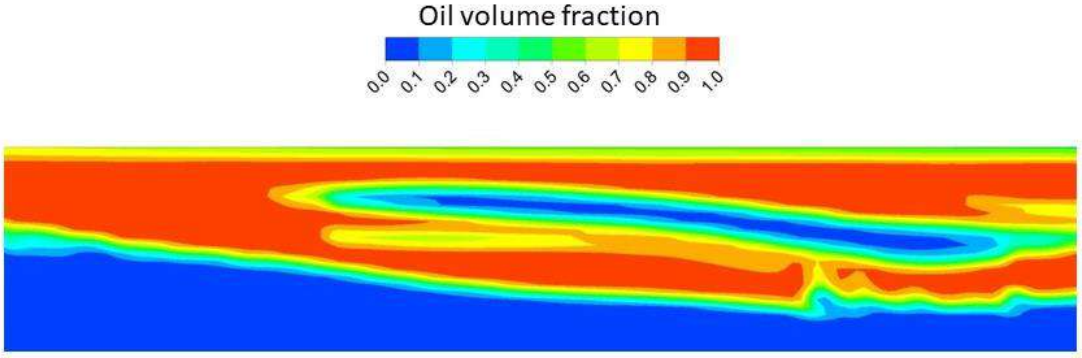

FIGURE 10. Simulation result of Oil Lumps in water (U_{so}: 0.12 m/s, U_{sw}: 0.81 m/s)

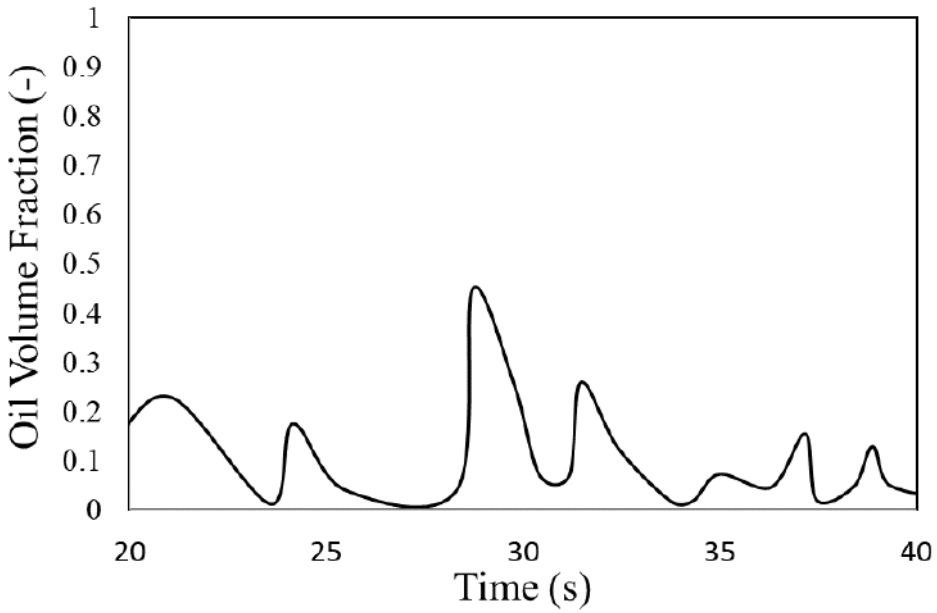

Figure 11. The oil volume fraction of Oil Lumps in water (U_{so}: 0.12 m/s, U_{sw}: 0.81 m/s)

Core annular flow

As the oil superficial velocity increases, the transition from oil plugs/lumps to core flow occurs. At the water superficial velocity = 0.12 m/s, and the oil superficial velocity = 0.18 m/s, the simulation flow pattern is characterized by annular flow or core flow, as shown in Figure 12. The flow pattern indicates that the oil flow passes through the water barrier because of increases in high oil inertia. For high oil viscosity, the viscous stress and interfacial stabilize the flow and counteract the deformation of the oil core flow. The gravitation force also plays a role in configurated oil-water flow patterns so that the water with higher density fluid tends to flow in the bottom of the pipe. Compared with the previous studies, the simulation results agree with the analysis of Shi and Yeung [9]. Next, Figure 13 shows that the oil volume fraction of core annular flow fluctuates periodically, mainly at the oil-water interfacial region. The increase of oil velocity leads to more oil-water interface fluctuation and forms a mixing zone, indicated as oil volume fraction fluctuation, as shown in Figure 14. Moreover, with the increase of oil and water velocity, the flow appears more fluctuated. The oil-water wave is shown in Fig. 14, while the oil volume fraction illustrates in Fig. 15. The flow was tended to be wavier than those of the lower velocity. It appears that the velocity influences the flow pattern as well as the physical properties.

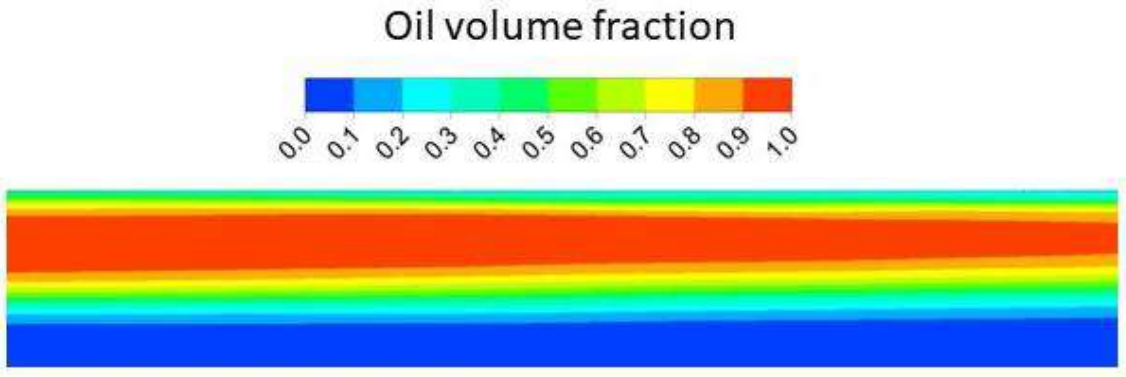

FIGURE 12. Simulation result of Core Annular flow (U_{so}: 0.12 m/s, U_{sw}: 0.18 m/s)

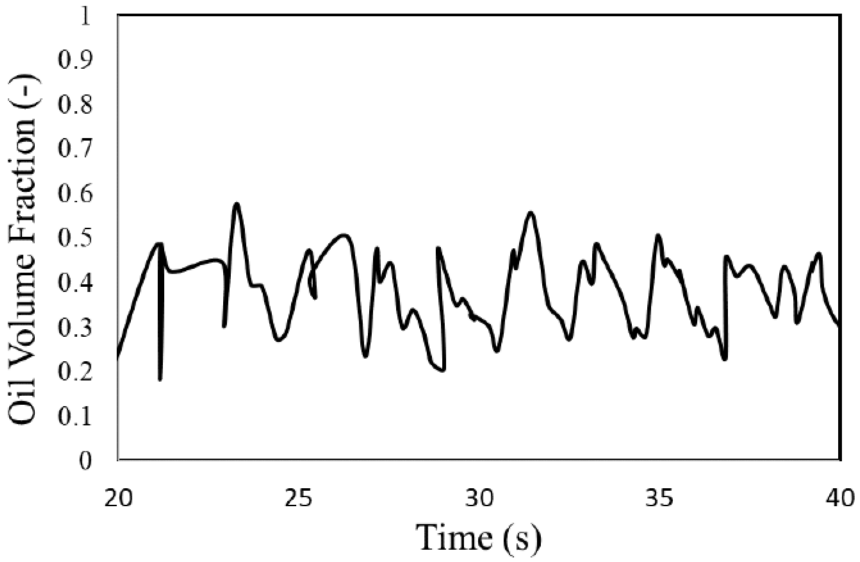

FIGURE 13. Oil volume fraction of Core Annular flow (U_{so}: 0.12 m/s, U_{sw}: 0.18 m/s)

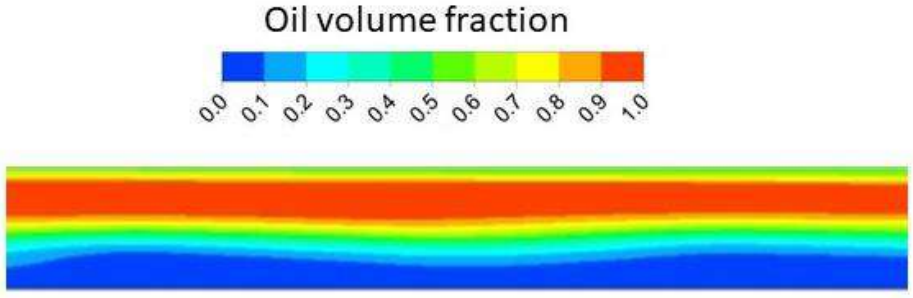

FIGURE 14. Simulation result of Core Annular flow (U_{so}: 0.4 m/s, U_{sw}: 0.6 m/s)

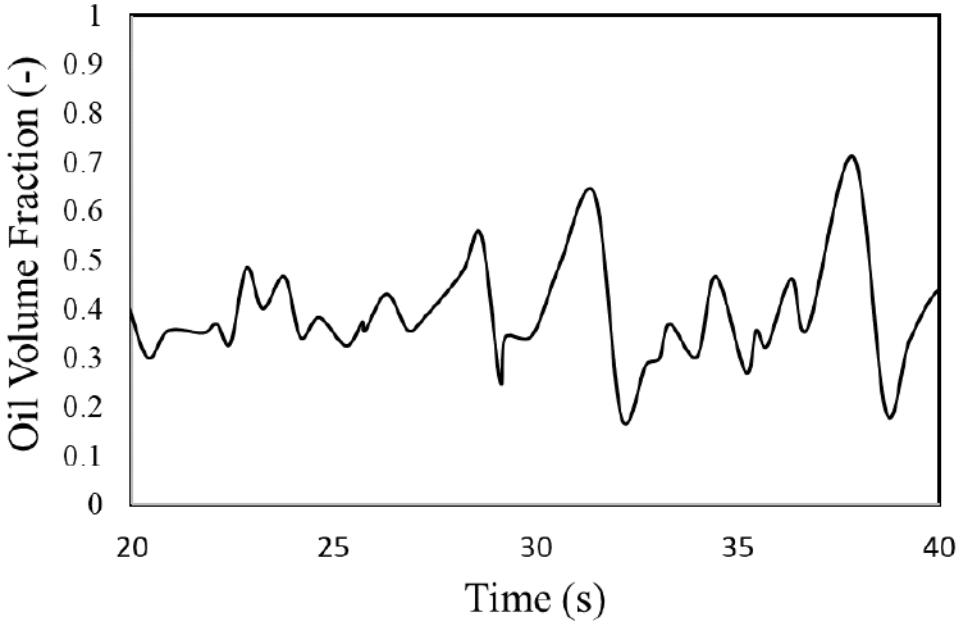

FIGURE 15. Oil volume fraction of Core Annular flow (U_{so}: 0.4 m/s, U_{sw}: 0.6 m/s)

Effect of Temperature

In this study, the water temperatures were varied as 300K and 373K. Figure 16 shows that the increasing temperature will change the flow pattern. The simulation result showed that the flow was changed from oil lumps in water to stratified due to the increasing temperature. As the increased of temperature, the viscosity of both oil and water became lower [7]. It also affected the surface tension between the flow. Hence, the fluids became less viscous, resulting in lower interfacial and friction force. The oil interface would be easier to break up, whereby the gravitational force dominates more. As a result, both fluids were easier to flow and produced stratified flow. In line with that, the oil volume fraction shown in Fig. 17 showed that the higher temperature flow has a more stable graph. It indicates the characteristic of stratified flow.

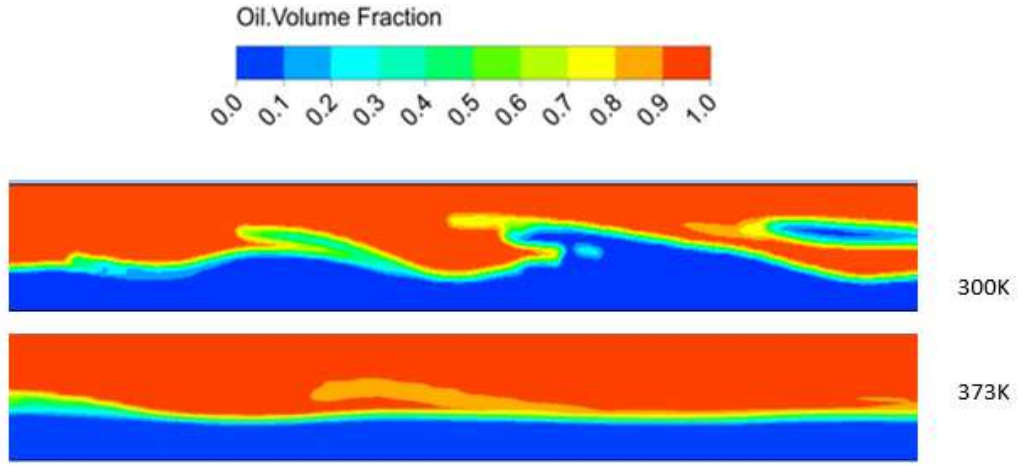

Figure 16. Comparison of flow at different temperature (U_{so}: 0.12 m/s, U_{sw}: 0.61 m/s)

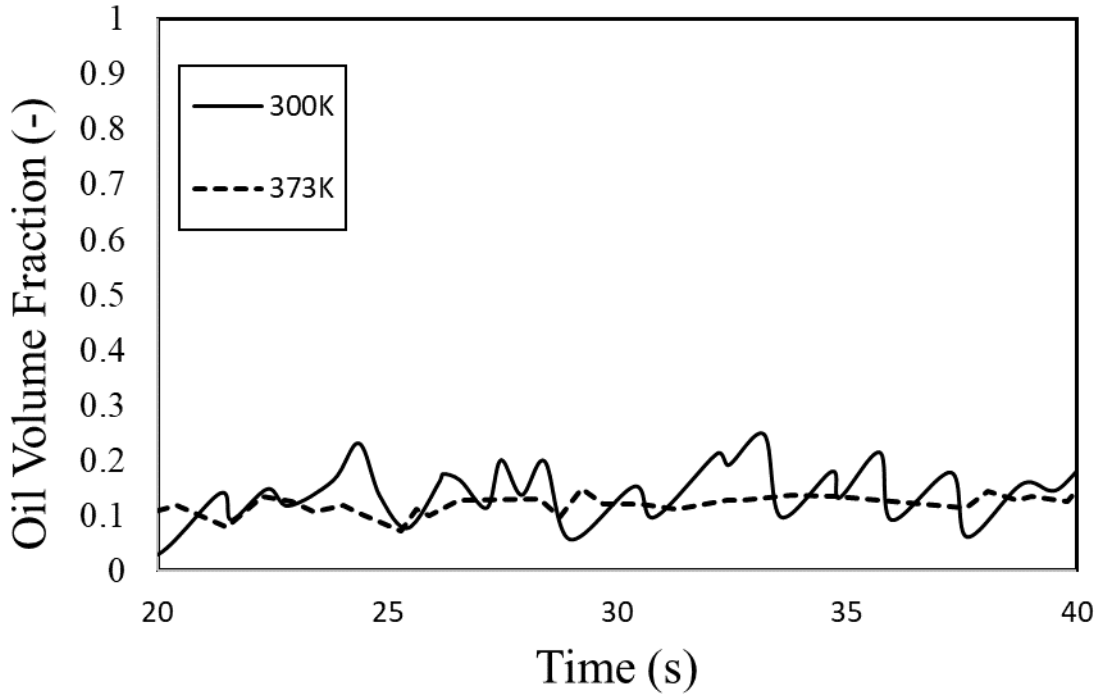

Figure 17. The Oil volume fraction of 300K and 373K

The viscosity value at the flow outlet relative to the Y-coordinate is illustrated in Fig. 18, while the temperature distribution is shown in Fig. 19. It explains the decrease of fluids' viscosity as the increase of temperature. Fig. 18 shows that the value of water viscosity is far lower than oil, where the value is nearly 0. Thus, the viscosity values between Y=0.1 and Y=0.5 are unnoticeably changed. From the CFD result, it can be drawn that the result of thermal-multiphase flow can be performed. It is clear that increasing temperature will reduce the fluids' viscosity. The ratio of viscosity is in accordance with the observed flow pattern. The more viscous fluids make it easier to flow, shifting the initial flow pattern into another form. In this study, the oil lumps in water flow converted into stratified flow due to the lower viscosity.

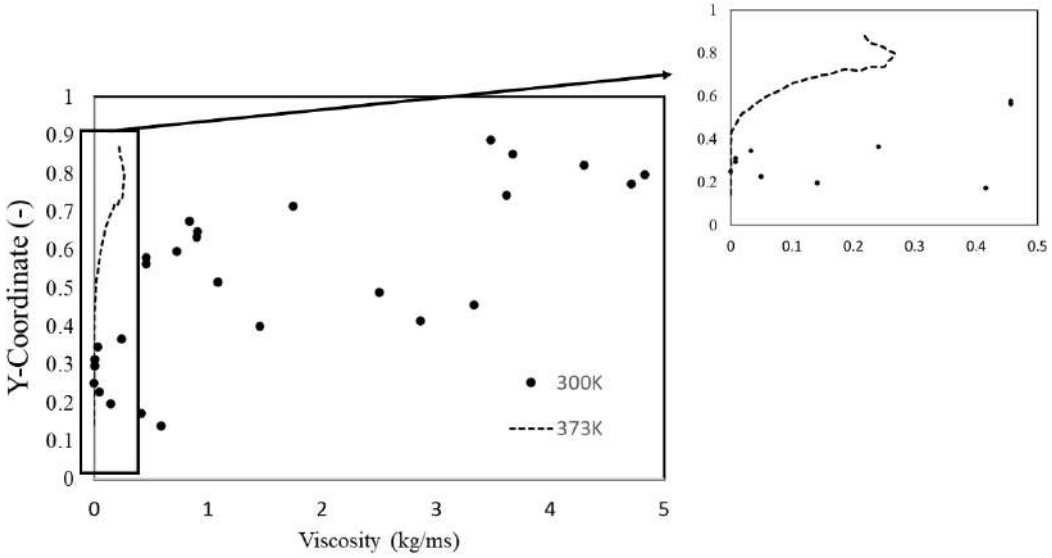

Figure 18. A plot of viscosity at Y-coordinate of 300K and 373K.

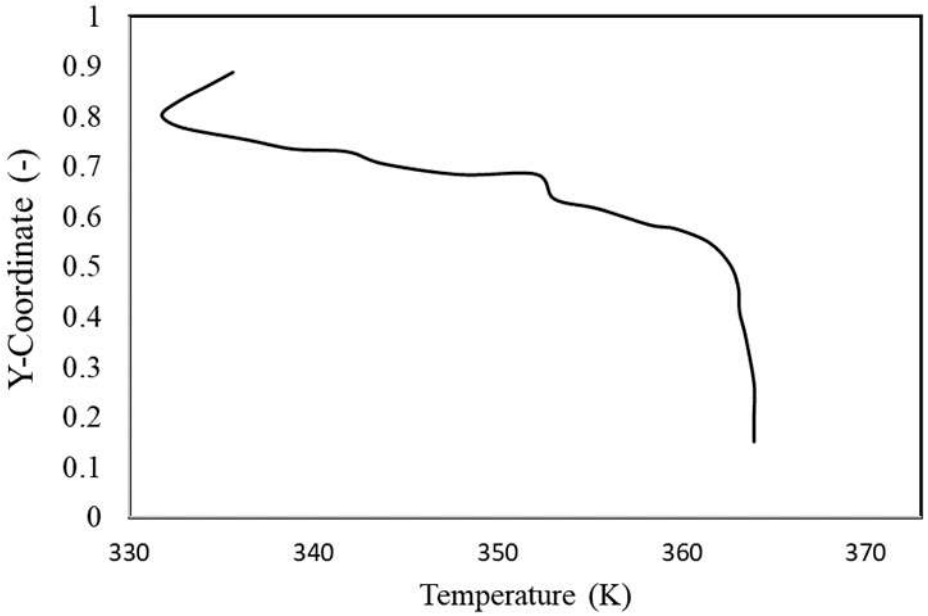

Figure 19. A plot of temperature distribution of the flow

CONCLUSION

Simulation of co-current water-oil multiphase flow in a horizontal pipe was conducted. The VoF model with SST $k-\omega$ model was utilized to investigate the flow. The brief of results is summarized as follows:

1. The simulation results showed a good agreement with those of experimental results. The numerical approach is able to investigate the practical case of oil-water flow. Furthermore, model improvement should be carried out, including 3D approximation.
2. The flow pattern obtained from the simulation can be divided into three basic categories: (1) oil plugs in water, (2) oil lamps in water, (3) core annular flow.
3. In this study, the CFD result clearly showed the changes flow due to the increased temperature. The oil lumps in the water flow were converted into the stratified flow as e result of the temperature effect. It concluded that CFD has the capabilities to simulate the multiphase flow in accordance with the temperature parameter.

ACKNOWLEDGMENTS

This work was carried out within the framework of the research project funded by the Ministry of Education and Culture, *Badan riset dan inovasi nasional* (project number: 01/K.2.2/Dik-LPPM/VI/2021) and the Internal Research Scheme, Institut Teknologi Dirgantara Adisutjipto (project number: Kep/107/VI/2021).

REFERENCES

1. P Angeli, G.F Hewitt, "Flow structure in horizontal oil–water flow, International Journal of Multiphase Flow.", Volume 26, 1117-1140 (2000)
2. Trallero, J.L., Sarica, C., and J.P. Brill. "A Study of Oil-Water Flow Patterns in Horizontal Pipes." SPE Prod & Fac 12 (1997)
3. Spedding, P.L.; Nguyen, V.T. "Regime map for air water two-phase flow." Chem. Eng. Sci. 35, 779–793 (1979)
4. H.Y. Kuntoro, A.Z. Hudaya, O. Dinaryanto, A.I. Majid, Deendarlianto, "An improved algorithm of image processing technique for film thickness measurement in a horizontal stratified gas-liquid two-phase flow", AIP Conferencee proceedings 1737, 040010 (2016)
5. O. Dinaryanto, A. Widyatama, A.I. Majid, Deendarlianto, "Image processing analysis on the air-water slug two-phase flow in a horizontal pipe", AIP Conference Proceedings 1737, 040011 (2016)
6. A. Al-Sarkhi, E. Pereyra, I. Mantilla, C. Avila, "Dimensionless oil-water stratified to non-stratified flow pattern transition", Journal of Petroleum Science and Engineering, Volume 151, Pages 284-291 (2017)
7. O. Alomair, M. Jumaa, A. Alkoriem, M. Hamed, "Heavy oil viscosity and density prediction at normal and elevated temperatures", J Petrol Explor Prod Technol 6, 253–263 (2016)
8. M. E. Charles, G. W. Govier, G. W. Hodgson, "The horizontal pipeline flow of equal density oil-water mixtures", Can. J. Chem. Eng., 39: 27-36. (1961)
9. M. Nädler, D. Mewes, "Flow induced emulsification in the flow of two immiscible liquids in horizontal pipes", International Journal of Multiphase Flow, Volume 23, Issue 1, Pages 55-68 (1997)
10. J. Shi and H. Yeung, "Characterization of liquid-liquid flows in horizontal pipes". AIChE J., 63: 1132-1143. (2017)
11. J. Shi, M. Gourma, H. Yeung, "A CFD study on horizontal oil-water flow with high viscosity ratio", Chemical Engineering Science, Volume 229, 116097 (2021)
12. Deendarlianto, M. Andrianto, A. Widyaparaga, O. Dinaryanto, Khasani, Indarto, "CFD Studies on the gas-liquid plug two-phase flow in a horizontal pipe", Journal of Petroleum Science and Engineering, Volume 147, Pages 779-787 (2016)
13. B. Jalaali and Pranowo, "The lattice Boltzmann meshless simulation of multiphase interfacial-instability", AIP Conference Proceedings 2248, 040007 (2020)
14. J. Tan, P. Luo, S. Vahaji, J. Jing, H. Hu, B. Yu, J. Tu, "Experimental investigation on phase inversion point and flow characteristics of heavy crude oil-water flow", Applied Thermal Engineering, Volume 180,115777 (2020)

15. K. A. Yuana, B. Jalaali, E. P. Budiana, Pranowo, A. Widyaparaga, Indarto, Deendarlianto, "Lattice Boltzmann simulation of the Rayleigh–Taylor Instability (RTI) during the mixing of the immiscible fluids", European Journal of Mechanics - B/Fluids, Volume 85, Pages 276-288 (2021)
16. B. Jalaali, M. R. E. Nasution, K. A. Yuana, Deendarlianto, O. Dinaryanto, "Investigating the effects of viscosity and density ratio on the numerical analysis of Rayleigh-Taylor instability in two-phase flow using Lattice Boltzmann method: From early stage to equilibrium state", Applied Mathematics and Computation, Volume 411, 126490 (2021)
17. J. Shi, M. Gourma, H. Yeung, "CFD simulation of horizontal oil-water flow with matched density and medium viscosity ratio in different flow regimes", Journal of Petroleum Science and Engineering, Volume 151, Pages 373-383 (2017)
18. P. B. Dehkordi, A. Azdarpour, E. Mohammadian, "The hydrodynamic behavior of high viscous oil-water flow through horizontal pipe undergoing sudden expansion—CFD study and experimental validation", Chemical Engineering Research and Design, Volume 139, Pages 144-161 (2018)
19. E. Burlutskii, "CFD study of oil-in-water two-phase flow in horizontal and vertical pipes", Journal of Petroleum Science and Engineering, Volume 162, Pages 524-531 (2018)
20. J.U. Brackbill, D.B. Kothe, C. Zemach, "A continuum method for modeling surface tension", Journal of Computational Physics, Volume 100, Issue 2, Pages 335-354 (1992)
21. ANSYS® Fluent, Fluent Theory Guide (2013). USA: ANSYS Inc
22. Peyret, R., "Handbook of Computational Fluid Mechanics". Academic Press Limited, USA. (1992)